An *ab initio* study of manganese atoms and wires interacting with carbon nanotubes

2004 J. Phys.: Condens. Matter 16 3647

(http://iopscience.iop.org/0953-8984/16/21/013)

INSTITUTE OF PHYSICS PUBLISHING JOURNAL OF PHYSICS: CONDENSED MATTER

J. Phys.: Condens. Matter **16** (2004) 3647–3661 PII: S0953-8984(04)76961-1

An *ab initio* study of manganese atoms and wires interacting with carbon nanotubes

Solange B Fagan[1], R Mota[2], Antônio J R da Silva[3] and A Fazzio[3]

[1] Departamento de Física, Universidade Federal do Ceará, CP 6030, CEP 60455-900, Fortaleza, CE, Brazil
[2] Departamento de Física, Universidade Federal de Santa Maria, CEP 97105-900, Santa Maria, RS, Brazil
[3] Instituto de Física, Universidade de São Paulo, CP 66318, CEP 05315-970, São Paulo, SP, Brazil

Received 26 February 2004
Published 14 May 2004
Online at stacks.iop.org/JPhysCM/16/3647
DOI: 10.1088/0953-8984/16/21/013

Abstract

A systematic study of Mn monomers, dimers, trimers, and wires interacting with an (8, 0) semiconductor single-wall carbon nanotube (SWCN) is presented. Spin-polarized total-energy *ab initio* calculations based on the density functional theory are used to describe the structural, electronic and magnetic properties of all studied systems. For Mn monomers, either outside or inside the nanotube, the most stable configuration is found to be over the centre of the hexagonal site. The most stable geometry for outside dimers presents the Mn atoms adsorbed directly on top of C atoms, when in a high-spin configuration, whereas for a low-spin configuration the Mn atoms are adsorbed on bond-centred sites at opposite sides of a hexagonal ring, with the Mn–Mn bond aligned in a diagonal direction relative to the tube axis in both cases. There are many low energy configurations (at $\simeq$0.1 eV above the lowest energy ones) at distinct orientations, for both the low and high energy configurations. For trimers, two kinds of Mn structures are investigated: compact or open. The compact trimers are found to be more stable than the open systems by approximately 1 eV/Mn atom. A monoatomic wire in a zig-zag configuration has a binding energy that is intermediate between the open and the compact trimers, independently of the spin configuration. For all the investigated Mn structures adsorbed on the SWCN, either high-spin (HS) or low-spin (LS), the interactions between Mn atoms and between Mn and C atoms become stronger as the Mn coordination number increases. The resulting magnetic moments for all adsorbed systems are found to be close to their original values for the corresponding free Mn structures.

(Some figures in this article are in colour only in the electronic version)

1. Introduction

Carbon nanotubes have attracted a lot of attention as a promising form of nanomaterials with multiple applications in nanodevices [1]. They have been extensively studied by both experimentalists and theorists since their discovery in a high-resolution transmission-electron microscopy experiment [2]. The production of SWCNs, with atomic structures that can be characterized by the chirality (n, m) that distinguishes different tube types [3], has permitted many propositions and new approaches for fundamental studies and technical applications, including interactions of these structures with different atoms and molecules on the tube surfaces. The possibility of modifying the properties of nanotubes by interactions with atoms and molecules has become a field of growing interest [1]. In particular, the combination of SWCNs with transition metal (TM) atoms is one of the promising routes towards new materials, and is considered of great interest in nanophysics, especially for spintronics. Although many theoretical [4–6] and experimental [7] works have studied the TM atoms interacting with SWCNs, most of the resulting physical, chemical and mechanical properties remains a challenging issue.

Among the TMs, Mn atoms are of great interest due to their unique characteristic of a half-filled d-shell, leading to intricate magnetic behaviours. Manganese, in bulk material, also presents the lowest bulk modulus and binding energy per atom among the 3d TMs [8]. Mn atoms interacting with a graphite surface have been investigated [9], but the SWCN adds a new feature to the problem. The curvature of the tube transforms the previous pure sp^2 hybridization into a mix between σ and π states, which leads to a different behaviour for Mn atoms on an SWCN when compared with a graphite sheet.

One important issue concerning TM atoms, and Mn in particular, is related to the possible wire formation on the tube surface [7]. This leads to the need to determine the conditions for either the occurrence of wires or, alternatively, clusters on the SWCN surface. Ti atoms, on the one hand, have a tendency to form wires whereas Au, on the other hand, are known to form clusters. For Mn, as well as Fe, these tendencies are not so clear-cut, requiring a much more detailed study of how these atoms interact with the tube surface [7]. The first step towards a comprehensive view is the complete understanding of the structural, electronic and magnetic properties of a single atom, dimers, trimers, and wires interacting with an SWCN. In a previous paper [5], we have presented preliminary results concerning the structural properties of Mn monomers and dimers adsorbed on SWCNs. In this work, a systematic study of these Mn structures adsorbed on an (8, 0) SWCN is performed through spin-polarized total-energy *ab initio* calculations. The next section details the procedure used in the calculations, which is followed by a discussion and presentation of our results. In the final section a summary of the main conclusions is given.

2. Calculation procedure

In order to investigate the structural, electronic and magnetic behaviours of Mn atoms interacting with SWCNs, *ab initio* total energy calculations, based on spin-polarized density functional theory, are employed [10]. We have used the SIESTA code [11], which performs full self-consistent calculations solving the Kohn–Sham (KS) equations. The KS orbitals are expanded using linear combinations of pseudoatomic orbitals proposed by Sankey and Niklewski [12]. In all calculations we have used a double-zeta basis set with polarization functions [11]. For the exchange and correlation term, the generalized gradient approximation [13] is used and the standard norm conserving Troullier–Martins pseudopotentials were adopted [14]. A cutoff of 150 Ryd for the grid integration was utilized to

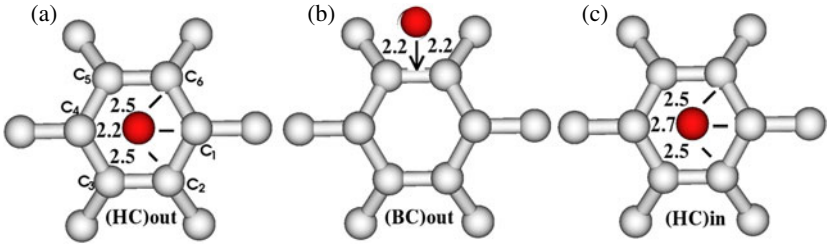

Figure 1. Final fully-relaxed structural configurations for the Mn tube configurations: (a) $(HC)_{out}$, (b) $(BC)_{out}$, and (c) $(HC)_{in}$. All distances are in Å.

represent the charge density. We have used 15 Monkhorst–Pack k-points for the Brillouin zone integration along the tube axis. Structural optimizations were performed using the conjugated gradient algorithm until the residual forces were smaller than 0.05 eV $Å^{-1}$.

For this investigation we used an (8, 0) SWCN, that is a semiconductor with a gap around 0.55 eV and diameter of 6.26 Å. In the supercell approximation with periodic-boundary conditions we have 64 C atoms and 1, 2 or 3 Mn atoms for structures with monomers, dimers and trimers, respectively, with a cell length in the growth direction of 8.52 Å. For Mn wires we use 32 C atoms and 2 Mn atoms in the supercell with a cell length in the growth direction of 4.26 Å. We use a lateral separation of 20 Å between tube centres, which prevents any tube–tube interaction for all studied systems.

3. Results and discussion

3.1. Monomers

The electronic configuration ($3d^5 4s^2$) on each Mn atom presents a majority spin with the 3d and 4s shells fully occupied and a minority spin with an occupied 4s state and an empty 3d shell state, making these states quite like the van der Waals molecules [15]. Besides that, the energy to promote the ground state configuration to $3d^6 4s^1$ is relatively high, which reduces the degree of s–d hybridization when Mn atoms are brought together. These behaviours have been assumed to be the main reason for the relatively weak binding and high magnetic moment in small Mn clusters [8, 15, 16].

To investigate the interaction of a single Mn atom adsorbed on the (8, 0) SWCN surface, four distinct sites were selected. These initial sites are described as follows:

(i) one with the atom approaching the centre of a hexagon from outside, labelled $(HC)_{out}$,
(ii) the same configuration from inside, $(HC)_{in}$,
(iii) along a direction perpendicular to the tube surface and pointing towards the middle of a C–C bond from outside, $(BC)_{out}$, and
(iv) directly above a C atom from outside, $(TOP)_{out}$.

All sites have been studied in such a way that the energies are minimized and all the atoms are allowed to relax.

Figure 1 shows schematically the final fully-relaxed structural configurations for the most stable ones: (a) $(HC)_{out}$, (b) $(BC)_{out}$, and (c) $(HC)_{in}$. As previously observed [5], the final configurations for (HC) positions present two sets (one with two and another with four) of similar bonds between the Mn and C atoms. These results are similar to those previously

Table 1. The binding energies (E_b), the total magnetic moments (M), including the tube contribution, as well as the contributions from 4s (m_s), 3d (m_d), and 4p (m_p) orbitals are shown for all the Mn configurations.

Mn position	E_b (eV)	M (μ_B)	m_s (μ_B)	m_d (μ_B)	m_p (μ_B)
$(HC)_{out}$	−0.50	5.2	0.7	4.5	0.2
$(BC)_{out}$	−0.20	5.1	0.8	4.4	0.2
$(TOP)_{out} \rightarrow (BC)_{out}$	−0.20	5.1	0.8	4.4	0.2
$(HC)_{in}$	−0.18	5.7	0.9	4.7	0.1

observed for Fe atoms [4] and are related to a mirror plane parallel to the tube axis that passes through the (HC) site and the C_1 and C_4 atoms. It is worth pointing out that, in contrast to the Fe atom case, the $(TOP)_{out}$ site is found to be unstable, tending to $(BC)_{out}$ (see table 1).

Table 1 presents the calculated binding energies, the total magnetic moments, as well as the contributions from 4s, 3d and 4p orbitals, for the studied sites. The binding energies, as usual, are calculated through the expression

$$E_b = E_{(\text{tube+Mn}(X))} - E_{(\text{tube})} - XE_{(\text{Mn})}, \tag{1}$$

where $E_{(\text{tube+Mn}(X))}$ is the spin-polarized total energy for the equilibrium structure of the (8, 0) tube plus the adsorbed X Mn atoms ($X = 1$, 2 and 3 for monomers, dimers, and trimers, respectively, and 2 for wires), $E_{(\text{tube})}$ is the energy of the isolated tube, and $E(\text{Mn})$ is the energy of an isolated Mn atom with the $3d^5 4s^2$ ground state configuration. Note that, from equation (1), the binding energies for dimers, trimers, and wires are obtained relative to the isolated atomic Mn. These values cover the Mn–Mn and Mn–C tube interactions and are not explicitly related to the isolated Mn structures of dimers, trimers or wires.

The most stable configuration is calculated to be the $(HC)_{out}$, similarly to what was obtained for Fe [4], as can be seen in table 1. For Fe, however, the binding energy is almost three times larger ($E_b^{(HC)_{out}}(\text{Fe}) = -1.4$ eV) than for Mn. Moreover, the energy difference between the most stable and the next most stable configurations is slightly higher for Mn (0.3 eV) than for Fe (0.25 eV), another difference being that this second most stable configuration for Fe is a $(BC)_{in}$ instead of a $(BC)_{out}$ as in Mn.

Duffy and Blackman [9] obtained as the most stable configuration for an Mn atom adsorbed on a graphite surface the site corresponding to what we have labelled (TOP) position, with a binding energy of −1.0 eV. More recently, Durgun *et al* [17] have obtained as the most stable position on the tube a result similar to ours ($(HC)_{out}$), with a binding energy of −0.4 eV.

In order to examine the stability of configurations with the TM atoms inside the nanotube, and in order to compare with available results for Fe in similar positions, we have only considered isolated Mn atoms interacting with the tube from inside. The position $(HC)_{in}$ was found to be the most stable one, but presenting a binding energy weaker than the corresponding outside configuration, as can be seen in table 1.

The contour plot for the $(HC)_{out}$ case is shown in figure 2(a) in a plane that passes through the C_5–Mn–C_2 atoms, whereas in figure 2(b) a similar plot is presented in a plane that passes through the C_4–Mn–C_1 atoms (see figure 1). Observe the larger charge density values between the Mn and the C_4 and C_1 atoms when compared to the C_5 and C_2 atoms (which is also consistent with the smaller equilibrium bond lengths). The opposite behaviour is observed for $(HC)_{in}$, with stronger interactions between the Mn–C_5 and Mn–C_2 bonds than between the Mn–C_4 and Mn–C_1 bonds, as can be seen in figures 2(c) and (d). This is a consequence of the fact that for the inside configuration, as opposed to the outside Mn structure, the bond lengths for the Mn–C_5 and Mn–C_2 bonds are the smaller ones, which is a result of the nanotube's curvature.

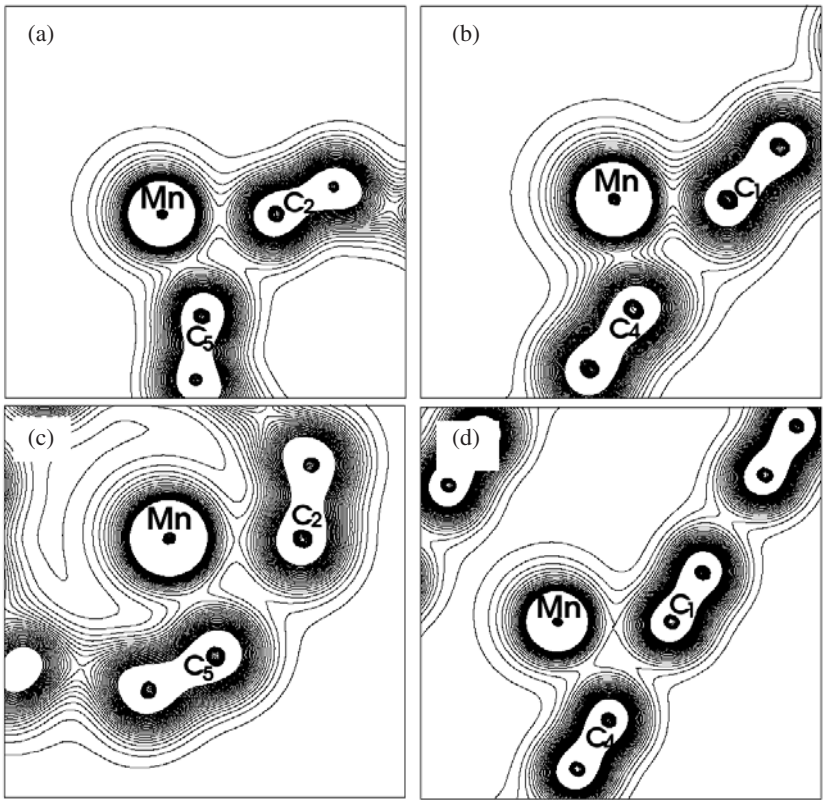

Figure 2. Contour plots of the total charge densities for both the $(HC)_{out}$ and the $(HC)_{in}$ configurations. For $(HC)_{out}$ the results are shown for (a) a plane that passes through the C_5–Mn–C_2 atoms and (b) a plane that passes through the C_4–Mn–C_1 atoms. For $(HC)_{in}$ the results are presented for (c) a plane that passes through the C_5–Mn–C_2 atoms, and (d) a plane that passes through the C_4–Mn–C_1 atoms. The outermost and innermost contour lines correspond to 0.0003 and 0.0099 e $Å^{-3}$, respectively, and the contour line spacing is 0.004 e $Å^{-3}$.

The band structures for the $(HC)_{out}$ configuration are shown in figure 3, together with the pure (8, 0) nanotube band structure shown in the left-hand side for comparison (figure 3(a)). The bands are presented separately for the majority (figure 3(b)) and minority (figure 3(c)) spins. The adsorption of Mn in the $(HC)_{out}$ configuration introduces two levels in the gap:

(i) one in the majority spin channel, with a dominant 4(sp) character, similar to what was previously observed for Fe atoms [4], and
(ii) another in the minority spin channel with a dominant 3d character.

Both these levels have a small dispersion that may be related to a small interaction between the Mn atoms in neighboring supercells. The majority spin bands with predominant Mn d-character appear resonant mostly located between 3.0 and 4.0 eV below the top of the valence band, as better seen in figure 3(e) for the projected densities of states (PDOS) onto the Mn atom for 4s plus 4p (4(sp)) and 3d. From figure 3(e) we can also see that most of the 3d Mn orbitals, for the minority spin states, are located inside the conduction band. It is observable too that there is a charge transfer from the Mn 4s to Mn 3d and 4p orbitals, leading to an effective $3d^{5.4}4s^{1.2}4p^{0.4}$ atomic configuration. Similar band structures are observed for $(BC)_{out}$.

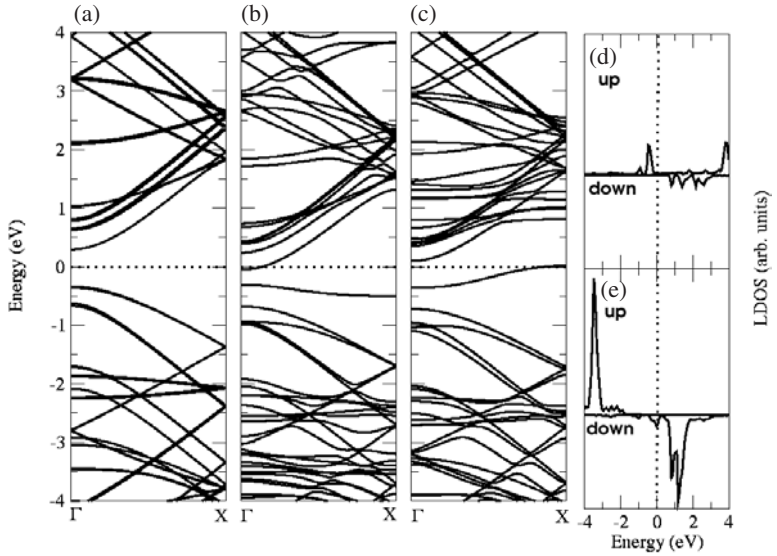

Figure 3. Electronic band structures for (a) pure (8, 0) SWCN, (b) majority spins and (c) minority spins, for the $(HC)_{out}$ configuration. (d) and (e) are the PDOS onto the Mn atom for 4s plus 4p and 3d orbitals, respectively, for both up (majority) and down (minority) spin channels. The dotted lines correspond to the Fermi level.

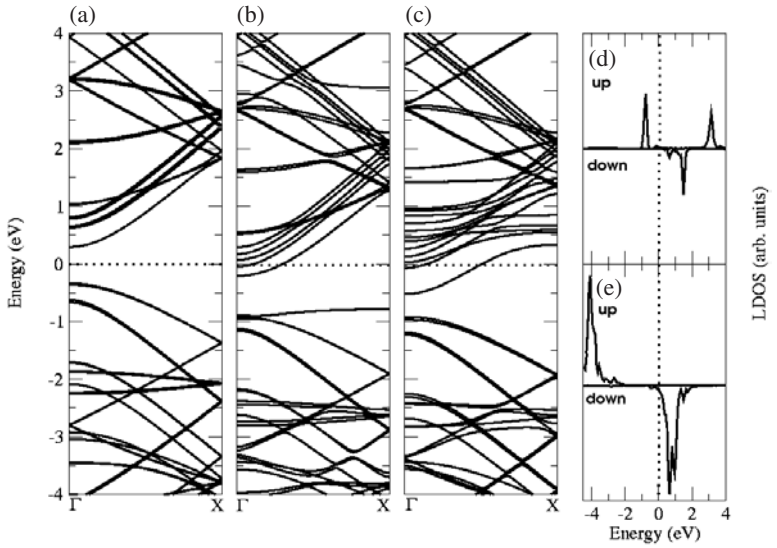

Figure 4. Electronic band structures for (a) pure (8, 0) SWCN, (b) majority spins and (c) minority spins, for the $(HC)_{in}$ configuration. (d) and (e) are the local PDOS onto the Mn atom for 4s plus 4p and 3d orbitals, respectively, for both up (majority) and down (minority) spin channels. The dotted lines correspond to the Fermi level.

The band structure for the Mn in the $(HC)_{in}$ site can be seen in figure 4. For the Mn inside the tube the final effective electronic structure configuration is similar to the $(HC)_{out}$ case, being $3d^{5.3}4s^{1.1}4p^{0.3}$. This is distinct from the Fe nanotube system, where an effective

$4s^0$ final configuration occurs for the inside structures [4]. The PDOS onto the Mn atom for 4s plus 4p and 3d for the $(HC)_{in}$ configuration are shown in figures 4(d) and (e), respectively, for majority and minority spins.

As shown in table 1, the total magnetic moment (M) for the Mn in the most stable $(HC)_{out}$ site is similar to what is obtained for an isolated atom (5.0 μ_B), whereas for the $(HC)_{in}$ it is slightly higher, 5.70 μ_B. These results are quite different from what was previously obtained [4] for an Fe atom in the same configurations, where the corresponding values are lower than the isolated atom limit (4.0 μ_B), being 3.90 and 2.36 μ_B, for the outside and inside sites, respectively. For the sake of comparison, for Mn in graphite, 6.0 μ_B was obtained for the total magnetization, with partial contributions of 4.5 μ_B from 3d, 1.1 μ_B from 4sp, and 0.4 μ_B from the C atoms [9]. For an Mn atom on the tube, previous results have obtained 5.49 μ_B [17].

It is noticeable to observe that Mn in the outside configuration ($3d^{5.4}4s^{1.2}4p^{0.4}$, as discussed above) corresponds to an approximately equal transfer of an average of $\simeq$0.8 4s down electrons to the 3d and 4p down orbitals. For the inside configuration ($3d^{5.3}4s^{1.1}4p^{0.3}$), an average of $\simeq$0.9 4s down electrons are equally transferred among the 4p, 3d and nanotube orbitals. On the other hand, for an Fe atom approaching the tube surface from outside ($3d^74s^1$), the 4s-down electron is basically transferred to the 3d-down orbital, whereas when it is inside ($3d^84s^0$), both 4s (up and down) electrons are transferred to the 3d down orbitals. Also, concerning the equilibrium distances to the tube, for the Mn atoms it is 2.2 Å for the outside and 2.5 Å for the inside sites, whereas for Fe it is 2.1 Å for both configurations.

3.2. Dimers

For the free-standing Mn dimer the 3d and 4s orbitals split into bonding and antibonding states, with the four s electrons filling both (up and down) states and not contributing to the net magnetic moment. There are two possible configurations for the d electrons:

(i) either the bonding and antibonding states spin up states are completely filled, leaving the spin down states empty, resulting in an HS order with net moment of 10 μ_B, or
(ii) they can all occupy the bonding orbitals, spins up and down, leading to an LS order with zero total moment.

In fact, this is a controversial issue, with many results conflicting with each other.

All the calculations agree that the bonding in Mn_2 is weak, but while some authors have reported, based on their experimental results, that an LS configuration coupled dimer is predicted for molecules in matrices [18], others [19] have concluded that Mn_2 is diamagnetic in its lowest state with spin unpairing occurring at high temperatures. Considering that there are no experiments on free Mn_2 clusters and that the matrix may affect the magnetic properties, the experimental scenario is still controversial, and there are still some questions concerning if the coupling is actually HS or LS configuration. In contrast, most of the theoretical calculations have found the Mn_2 to be HS order, with a total magnetic moment of 10 μ_B, but with binding energies presenting great discrepancies among them. This variety of results, extremely dependent on the adopted methods and approximations, is due to the weak bond between the two atoms, making the obtained results direct consequences of the choice of basis function and level of correlations.

Our calculations demonstrate that there are, in fact, three competitive states for free-standing Mn dimers: two in HS configuration (two minima binding energies, one with -0.31 eV and interatomic distance of 3.14 Å and the other with -0.26 eV and a shorter distance of 2.62 Å) and a third one in an LS configuration (intermediate binding energy of

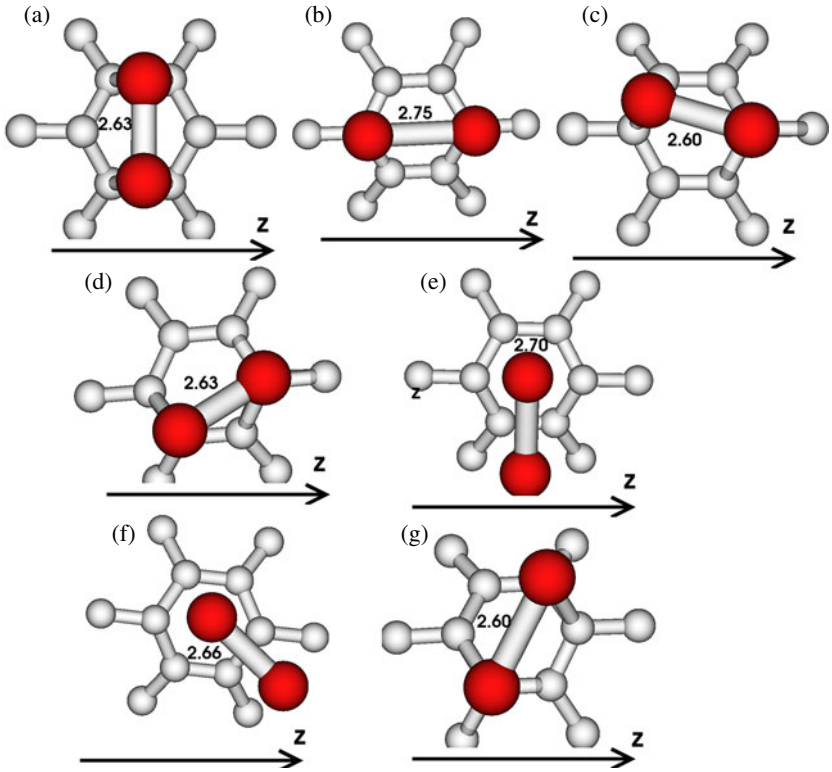

Figure 5. Final fully-relaxed geometries for the most stable high-spin configurations for Mn dimers adsorbed on the (8, 0) SWCN.

−0.27 eV and an interatomic distance of 3.10 Å). These results would help to elucidate why it seems to be so difficult to reach a final conclusion about HS and LS order solutions, making the Mn_2 dimers one of the most complex in terms of number of stable and metastable magnetic and geometric states that they can assume.

Figure 5 presents the final fully-relaxed structural configurations for several studied dimers adsorbed on carbon tubes. In general, the binding energies do not differ too much one from another. Among the studied sites, the most stable configuration for HS configuration Mn_2 approaching from outside is determined, in accordance with table 2, to be the diagonal (TOP)–(TOP), as can be seen in figure 5(g). For the Mn–Mn distances, as well as for the binding energies, total magnetic moments, magnetic moments per atom and tube magnetic moments, small fluctuations are observed. In our case, we have obtained as the equilibrium position (Mn–Mn distance) for the most stable dimer adsorbed on the tube 2.60 Å, which value is closer to the local minimum (2.62 Å) than to the total minimum (3.14 Å) for the free HS configuration dimer.

Observe that the binding energies per Mn atom in dimers adsorbed on tube, as shown in table 2, are significantly higher (at least 0.71 eV) than the corresponding values obtained for monomers (maximum of 0.50 eV). To illustrate that, in figure 6(c) the contour plots are shown for the (TOP)–(TOP) HS order case in a plane that passes through the Mn atoms. The interaction between Mn and Mn atoms, when they are adsorbed on the tube surface, gets stronger compared with when they are isolated (in figure 6(a) the contour plot for the free

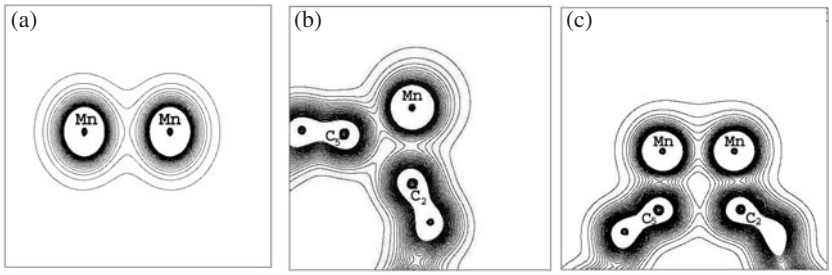

Figure 6. Contour plots for the total charge density for HS configurations for (a) Mn_2 isolated, (b) Mn monomer on the tube surface, and (c) Mn dimer adsorbed on SWCN in the most stable structure corresponding to figure 5(g). The outermost and innermost contour lines correspond to 0.0003 and 0.0099 e $Å^{-3}$, respectively, and the contour line spacing is 0.004 e $Å^{-3}$.

Table 2. The binding energies (in eV) per Mn atom (E_b), the Mn–Mn distances (in Å), the total magnetic moments (M), the Mn atom magnetic moments and the tube magnetic moments (all in μ_B) for all the HS order for Mn dimers adsorbed on an SWCN surface for the Mn_2 tube positions as indicated in figure 5.

Position	E_b	d_{Mn-Mn}	M	$M_{Mn\text{-atom}}$	M_{tube}
(a)	−0.80	2.63	8.5	4.5	−0.5
(b)	−0.73	2.75	9.6	4.9	−0.2
(c)	−0.77	2.60	8.6	4.5	−0.4
(d)	−0.71	2.63	9.0	4.8	−0.6
(e)	−0.71	2.70	9.9	4.9	0.1
(f)	−0.82	2.66	9.8	4.8	0.2
(g)	−0.85	2.60	9.0	4.6	−0.2

magnetic Mn dimer is presented for comparison). The interaction between Mn and C atoms is also stronger, characterized by a larger value of the charge density between the Mn and C atoms, compared with the corresponding values for monomers (see figure 6(b)). These results indicated that, for Mn atoms, the interaction strengths enhance when the number of bonds is increased.

Figure 7 shows the PDOS onto the Mn atoms for 4s plus 4p orbitals (dashed curves) and 3d orbitals (continuous curves), for spins up and down as indicated in the figure. This figure helps us to understand the role played by the HS configuration dimer in the nanotube. The effective configuration for each Mn atom in this configuration is $4(sp)^{1.4}3d^{5.3}$. For the 4s plus 4p orbitals, in contrast to the free dimer that has both the 4s up and down spins occupied, we can observe that there is a spin polarization, with the majority of the down spin states located above the Fermi energy and being therefore unoccupied. For 3d orbitals, a small contribution of the spin down levels to the occupied states is noticeable, whereas in the free dimer these levels are totally unoccupied.

The final fully-relaxed structural configurations for several studied LS order Mn dimers adsorbed on SWCN are shown in figure 8. The most stable configuration, as shown in table 3, is (BC)–(BC) (see figure 8(g)), also in a diagonal position relative to the tube axis direction, and it corresponds to the minimum Mn–Mn distance among the cases studied. In general, the binding energies are slightly higher than the corresponding values for HS order. To compare with a free LS order Mn_2 dimer, the calculated binding energy is −0.27 eV and the equilibrium Mn–Mn distance is 3.10 Å. Figure 9 shows the PDOS on the Mn atoms for the diagonal

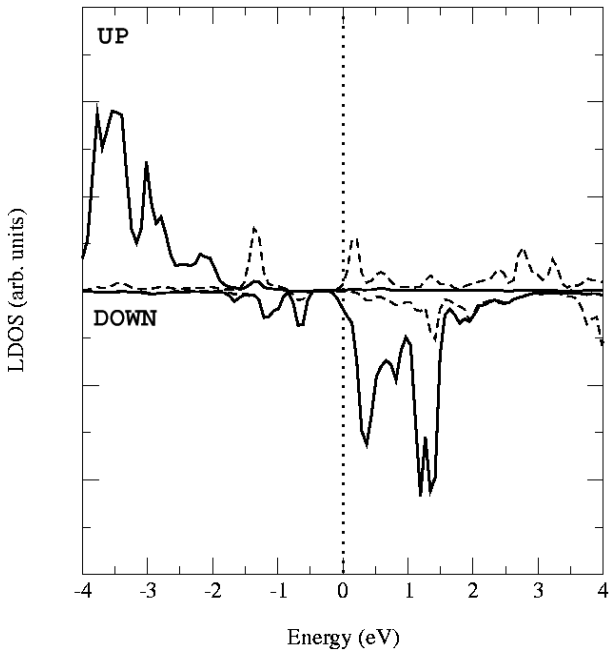

Figure 7. PDOS for the Mn atoms in dimers adsorbed on the SWCN surface in a diagonal (TOP)–(TOP) position with HS configuration (figure 5(g)). The dashed curves indicate the 4s plus 4p orbitals and the continuous curves indicate the 3d orbitals. The vertical dotted line corresponds to the Fermi energy.

Table 3. The binding energies (in eV) per Mn atom (E_b), the Mn–Mn distances (in Å), the total magnetic moments (M), the Mn atom magnetic moments and the tube magnetic moments (all in μ_B) for all the LS order for Mn dimers adsorbed on an SWCN surface for the Mn_2 tube positions as indicated in figure 8.

Position	E_b	d_{Mn-Mn}	M	$M_{Mn\text{-atom}}$	M_{tube}
(a)	−0.77	2.58	0.2	±5.1	0.2
(b)	−0.81	2.63	0.0	±4.8	0.0
(c)	−0.87	2.58	0.0	±4.8	0.0
(d)	−0.80	2.58	0.2	±5.0	0.2
(e)	−0.75	2.67	−0.3	+5.0/−5.1	−0.2
(f)	−0.90	2.64	0.0	±5.0	0.0
(g)	−0.91	2.53	0.0	±4.8	0.0

(BC)–(BC) Mn dimer adsorbed on an SWCN surface, showing that the system has a total zero magnetic moment. Each Mn, however, has an effective configuration $4(sp)^{1.4}3d^{5.5}$, which is similar to the one in the HS case. This indicates that the Mn magnetic moments are similar in both cases (LS and HS), but in the LS state they are coupled in an antiparallel configuration. This can also be seen in tables 2 and 3, where it is shown that the resulting magnetic moments for the adsorbed LS order dimers are similar to the HS order dimers, being also similar to the corresponding free dimer values.

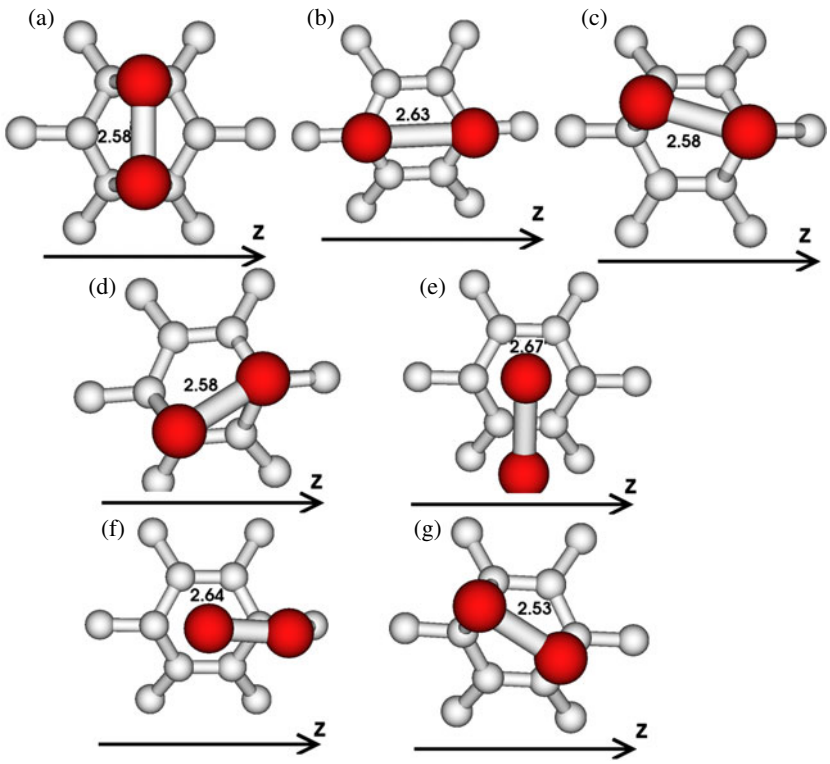

Figure 8. Final fully-relaxed structural configurations for the LS Mn_2 tube configurations.

3.3. Trimers and wires

To analyse the trimers, the choice of the studied structures was limited by the supercell method, in such a way that the Mn atoms of one cell do not interfere with the (periodically repeated) Mn atoms of the next cell. Then, starting from the most stable dimers compatible with that limitation, two trimer structures seem to be appropriate for our discussion. One is a compact structure, labelled (BC)–(HC)–(BC), based on a (BC)–(BC) dimer along a direction perpendicular to the tube axis direction, with the third Mn atom, above the same carbon ring, occupying a position along the direction perpendicular to the centre of the hexagon ((HC) position, as described before). Another, more open structure, labelled (BC)–(BC)–(BC), is also based on the same (BC)–(BC) dimer, but with the third Mn atom above the middle of a C–C bond in the next consecutive carbon ring. Figure 10 shows these structures in different perspectives for the HS (figures 10(a) and (b)) and LS (figures 10(c) and (d)) cases, respectively.

According to the results shown in table 4, the binding energies for the (BC)–(HC)–(BC) are much (almost twice) higher than for the (BC)–(BC)–(BC) structures, for both HS and LS configuration cases.

Figure 11 shows the contour plots for the Mn_3 isolated (figures 11(a) and (b)) and adsorbed on SWCN (figures 11(c) and (d)) for the more compact and more open structures in HS configurations. It is possible to observe the interactions and how they change with the presence of the tube for each case. For both cases, the interactions among the Mn atoms are enhanced when the coordination number per atom increases, a behaviour that is similar to what has already been observed for dimers. Nevertheless, the enhancement is clearly much higher for

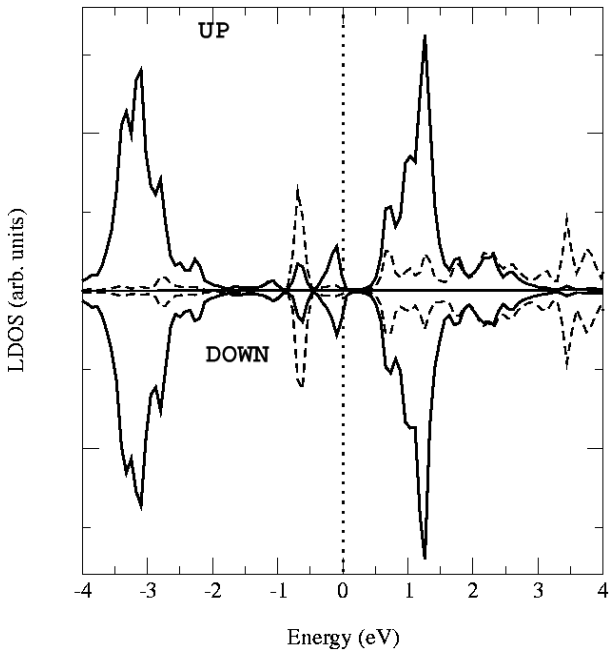

Figure 9. PDOS for the Mn atoms in dimers adsorbed on an SWCN surface in a diagonal (BC)–(BC) position with LS configuration. The dashed curves indicate the 4s plus 4p orbitals and the continuous curves indicate the 3d orbitals. The vertical dotted line corresponds to the Fermi energy.

Table 4. The binding energies (in eV) per Mn atom (E_b), Mn–Mn distances (in Å), and the total magnetic moments (M), for the most stable configurations for monomers, dimers, trimers and wires for HS and LS configurations.

Mn structure	E_b	d_{Mn-Mn}	M
Monomer	−0.50	—	5.2
Dimer-HS	−0.85	2.60	9.1
Dimer-LS	−0.91	2.53	0.0
Compact-trimer-HS	−1.50	2.48/2.60	11.2
Compact-trimer-LS	−1.49	2.46/2.58	4.0
Open-trimer-HS	−0.85	2.73	13.6
Open-trimer-LS	−0.85	2.70	4.3
Wire-HS	−1.20	2.60/2.65	8.3
Wire-LS	−1.26	2.60/2.65	0.1

the first (compact) than for the second (open) case, which is compatible with the binding energies shown in table 4. Observe that for both the open and compact structures, the Mn atom in the middle (labelled 2 in the figures) presents very small interaction with the tube, but in the compact structure this atom is much more bound to the other Mn atoms (labelled 1 and 3) than in the open structure. Exactly the same behaviour is observed for the LS configuration (observe that the differences in binding energies between the two spin configurations for the same Mn_3 structure—compact or open—are negligible).

The atomic configuration for an HS wire adsorbed on the tube can be seen in figure 12. Again, it is observed that the interaction among the Mn atoms is enhanced when the

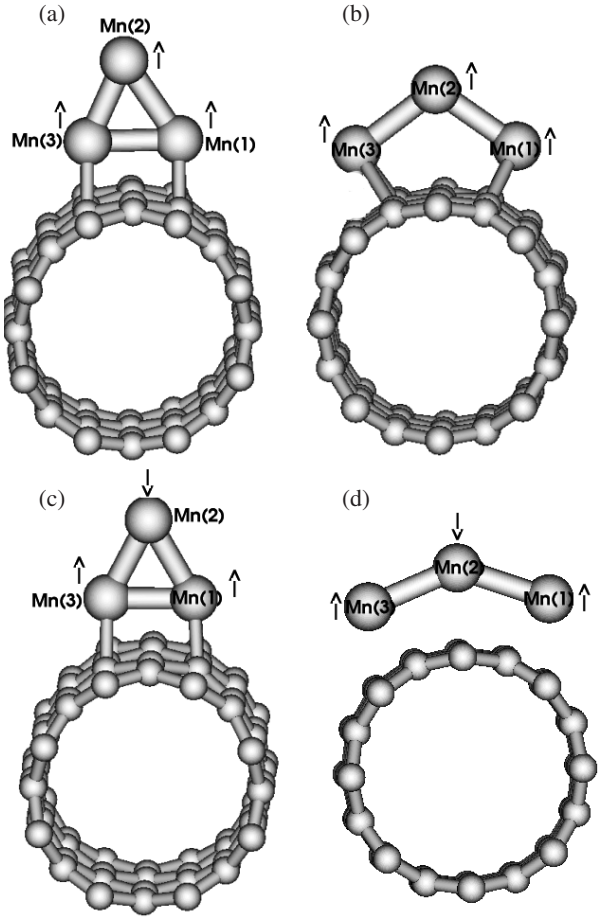

Figure 10. Trimers adsorbed on the tube surface for the HS configuration (a) compact and (b) open structures, and LS configuration (c) compact and (d) open structures. The arrows indicate the magnetic order for each Mn atom, up or down.

coordination number per atom increases, as previously observed for dimers and trimers. The contour plots for the total charge densities for the isolated wire, as well as when it is adsorbed on the tube surface, are shown in figures 12(b) and (c), respectively. A monoatomic wire in a zig-zag configuration has a binding energy, as can be seen in table 4, that is intermediate between the open and compact trimers, independent of the spin configuration.

4. Summary and conclusions

Considering that the investigation of TMs adsorbed on SWCNs is certainly of great current interest in nanophysics, this paper presents a systematic study of the structural, electronic and magnetic properties of Mn monomers, dimers, trimers and wires interacting with an (8, 0) SWCN. The final fully-relaxed structural configurations and the equilibrium distances from the tube surface to the Mn atoms were determined for all the systems under investigation. In all studied systems the resulting relaxed structures of the SWCN have a small radial distortion due to the presence of Mn atoms; this value is less than 2% of the isolated SWCN radius.

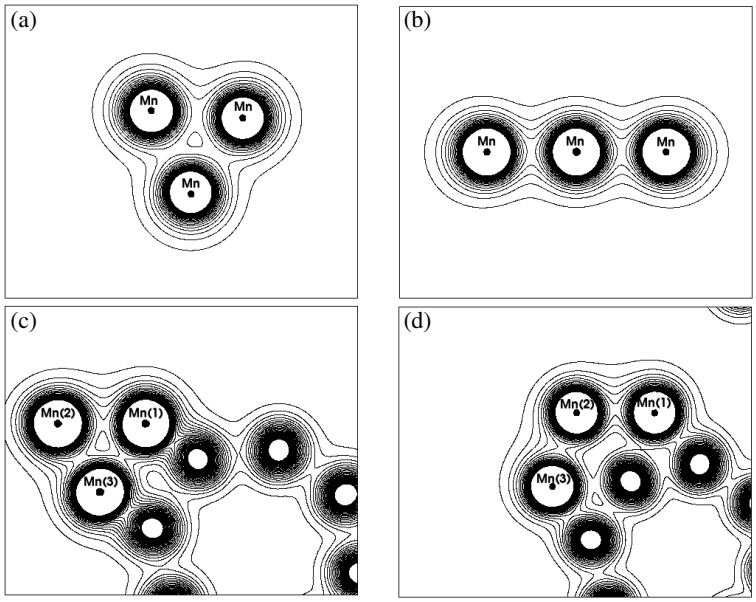

Figure 11. Contour plots for the total charge densities for: isolated Mn_3 in a compact (a) and open (b) structure, and for the trimers structure adsorbed on SWCN surface (c) compact and (d) open configuration. All systems shown are for HS configurations. The outermost and innermost contour lines correspond to 0.0003 and 0.0099 e $Å^{-3}$, respectively, and the contour line spacing is 0.004 e $Å^{-3}$.

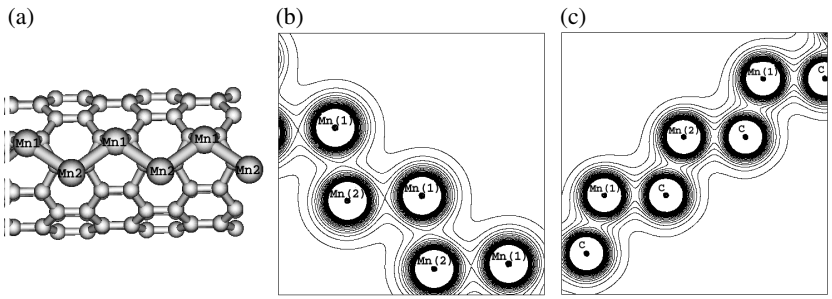

Figure 12. (a) Atomic configuration for an HS ordered wire adsorbed on the tube surface. Total charge density contour plots for (b) an isolated wire and (c) a wire adsorbed on the tube surface. The outermost and innermost contour lines correspond to 0.0003 and 0.0099 e $Å^{-3}$, respectively, and the contour line spacing is 0.004 e $Å^{-3}$.

For monomers the (HC) geometry was found to be the most stable structure, for both inside and outside configurations. The binding energies are smaller when compared to the values previously obtained for Fe monomer. In terms of electronic structure, it was demonstrated that for Mn monomer adsorbed from outside an effective $3d^{5.4}4s^{1.2}4p^{0.4}$ configuration is obtained, different from the $3d^74s^1$ calculated previously for Fe monomer. Similarly, for Mn from inside an effective $3d^{5.3}4s^{1.1}4p^{0.3}$ configuration results, also contrasting with the $3d^84s^0$ for Fe in a corresponding configuration. The total magnetic moment for the outside configuration was found to be similar to that for the atomic configuration, and for the inside configuration slightly higher.

For Mn dimers on an SWCN it is shown to be important to consider both HS as well as LS configurations, since they present competitive energies. In the HS configuration, the diagonal with respect to the tube axis (TOP)–(TOP) geometry was found to be the most stable one. For the LS case, the most stable configuration was (BC)–(BC), also in a diagonal position relative to the tube axis direction. In general, no substantial differences in binding energies were observed for all the studied dimer configurations. It is worth pointing out that the (TOP) site was found to be unstable for the monomer, demonstrating that, in general, the dimer configurations are not simply related to the isolated monomer structures. The binding energies per atom for the most stable adsorbed dimer on the tube (-0.85 eV) is larger than the sum of the corresponding monomer binding energy (-0.50 eV) plus the binding energy per atom for the free Mn dimer (around -0.15 eV). The interaction between Mn–Mn atoms on tube becomes stronger when compared to the isolated molecule. Moreover, for dimers the Mn tube is enhanced when compared to monomers. Then, for both HS as well as LS configurations, the processes of forming dimers on the tube are favourable when compared to two separated monomers.

With respect to trimer configurations, two appropriate structures were chosen, labelled compact ((BC)–(HC)–(BC)) and open ((BC)–(BC)–(BC)). The calculated binding energies are higher for the compact than for open structures. For both cases, it was observed that the interactions among the Mn atoms are enhanced when the coordination number increases, with the enhancement being clearly higher for the compact than for the open configuration. These results are valid for HS order as well as for LS spin configurations. Concerning the Mn wire, its binding energy is intermediate between the open and the compact trimers, independent of the spin configuration. Finally, we obtain that the magnetic moments for all adsorbed systems are very similar to their corresponding free Mn structures.

Acknowledgments

We would like to thank the CENAPAD-SP for the computer time. This research was supported by CNPq, CAPES, FAPERGS and FAPESP.

References

[1] Dai H 2002 *Surf. Sci.* **500** 218
[2] Iijima S 1991 *Nature* **354** 36
[3] Dresselhaus M S, Dresselhaus G and Avouris P 2001 *Carbon Nanotubes* (Berlin: Springer)
[4] Fagan S B, Mota R, da Silva A J R and Fazzio A 2003 *Phys. Rev.* B **67** 205414
[5] Fagan S B, Mota R, da Silva A J R and Fazzio A 2003 *Physica* B **340–342** 982
[6] Andriotis A N, Menon M and Froudakis G 2000 *Phys. Rev. Lett.* **85** 3193
Yang C-K, Zhao J and Lu J P 2003 *Phys. Rev. Lett.* **90** 257203
Lee Y H, Kim S G and Tomanek D 1997 *Phys. Rev. Lett.* **78** 2393
Kong K, Han S and Ihm J 1999 *Phys. Rev.* B **60** 6074
[7] Zhang Y, Franklin N W, Chen R J and Dai H 2000 *Chem. Phys. Lett.* **331** 35
[8] Pederson M R, Reuse F and Khanna S N 1998 *Phys. Rev.* B **58** 5632
[9] Duffy D M and Blackman J A 1998 *Phys. Rev.* B **58** 7443
[10] Hohenberg P and Kohn W 1964 *Phys. Rev.* **136** B864
Kohn W and Sham L J 1965 *Phys. Rev.* **140** A1133
[11] Ordejón P, Artacho E and Soler J M 1996 *Phys. Rev.* B **53** 10441
Sánchez-Portal D, Artacho E and Soler J M 1997 *Int. J. Quantum Chem.* **65** 453
[12] Sankey O F and Niklewski D J 1989 *Phys. Rev.* B **40** 3979
[13] Perdew J P, Burke K and Ernzerhof M 1996 *Phys. Rev. Lett.* **77** 3865
[14] Troullier N and Martins J L 1991 *Phys. Rev.* B **43** 1993
[15] Nayak S K, Rao B K and Jena P 1998 *J. Phys.: Condens. Matter* **10** 10863
[16] Desmarais N, Reuse F A and Khanna S N 2000 *J. Chem. Phys.* **112** 5576
[17] Durgun E, Dag S, Bagci V M K, Gülseren O, Yildirim T and Ciraci S 2003 *Phys. Rev.* B **67** 201401
[18] Cheesseman M, Van Zee R J and Weltner W 1989 *J. Chem. Phys.* **91** 2748
[19] Baumann C A, Van Zee R J, Bhat S and Weltner W 1983 *J. Chem. Phys.* **78** 190